

# Implications of the heavy Higgs induced single-top, same-sign top and triple-top productions at the LHC

Tanmoy Modak

*Institut für Theoretische Physik, Universität Heidelberg, 69120 Heidelberg, Germany*

In this brief review we study the discovery potential of heavy Higgs induced single-top, same-sign top and triple-top quark productions at the Large Hadron Collider (LHC). The context is general two Higgs doublet model where such processes can be induced by additional Yukawa couplings and sub-Tev Higgs bosons. We show that these processes can be discovered at the ongoing or future high luminosity LHC run. Discovery of these multi-top productions may shed light on the mechanism behind baryogenesis or cosmic inflation.

## I. INTRODUCTION

The study of top quark productions is a staple program at the LHC. As a proton-proton collider LHC produces top-quarks abundantly and provides unique window to study multi-top quark productions. In the early part of Run-1 ATLAS and CMS collaborations swiftly rediscovered  $t\bar{t}$  production [1, 2]. Subsequently LHC also measured the single-top productions both in the  $t$ - [3–6] and  $tW$  [7–10] channels. Searches for the subdominant  $s$ -channel single-top production are also performed by both the collaborations [11–13]. On the other hand, the triple-top production is at merely few fb in the Standard Model (SM) [14] but the QCD initiated four-top production is at  $\mathcal{O}(10)$  fb. While none of the experiments have covered the SM triple-top in their search programs so far however the four-top productions are searched by ATLAS [15, 16] and CMS [17, 18].

Multi-top productions are also possible in the minimal extensions of the SM such as the two Higgs doublet model (2HDM) [19, 20]. After the discovery of the 125 GeV Higgs boson  $h$  [21] presence of additional Higgs doublet seems more plausible. In such model in addition to the observed  $h$  boson heavy additional scalars  $A$  and  $H$  or the charged Higgs boson  $H^\pm$  may also induce different top quark productions. Indeed, extensive efforts have been directed towards these heavy Higgs induced multi-top quark productions e.g.  $pp \rightarrow A/H \rightarrow t\bar{t}$  [22–30],  $pp \rightarrow t\bar{t}A/H \rightarrow t\bar{t}t\bar{t}$  [18, 23, 31–34], and  $pp \rightarrow t\bar{t}H^+(b) \rightarrow t\bar{t}b(b)$  [35–50] at the LHC.

In this brief review we focus on some additional multi-top productions in the context of general 2HDM (g2HDM). In the absence of any discrete symmetry both the doublets in g2HDM couple with up- and down-type fermions. After diagonalization of the fermion mass matrices two different Yukawa couplings  $\lambda_{ij}^F = (\sqrt{2}m_i^F/v)\delta_{ij}$  (with  $v \simeq 246$  GeV) and  $\rho_{ij}^F$  emerge with  $F$  denoting up- and down-type quarks and charged-leptons. While, the  $\lambda_{ij}^F$  matrices are real and diagonal but the  $\rho_{ij}^F$  are in general complex and nondiagonal.

It has been shown that successful electroweak baryogenesis (EWBG) is possible for sizeable complex  $\rho_{\tau\tau}$  [51],  $\rho_{tt}$  and  $\rho_{tc}$  [52]<sup>1</sup>, and  $\rho_{bb}$  [57]. Motivated by this Refs. [58, 59] (for similar discussion see also Refs. [60–65]) have analyzed the possibility of discovering  $cg \rightarrow tA/tH \rightarrow t\bar{t}\bar{c}$  (denoted as same-sign top) process at the LHC. The process is induced by  $\rho_{tc}$  coupling and can be searched via  $pp \rightarrow tA/tH + X \rightarrow t\bar{t}\bar{c} + X$  ( $X$  is inclusive activity) followed by semileptonic decay of both the top quarks constituting a clean same-

<sup>1</sup> Similar mechanisms are also discussed in Refs. [53–56].

sign dilepton signature. Furthermore, if both  $\rho_{tc}$  and  $\rho_{tt}$  are nonvanishing one may have  $cg \rightarrow tA/tH \rightarrow tt\bar{t}$  (triple-top) [58, 66, 67] and  $cg \rightarrow bH^+ \rightarrow bt\bar{b}$  (single-top) production. At the LHC the former process can be searched via  $pp \rightarrow tA/tH + X \rightarrow tt\bar{t} + X$  with all three top quarks decaying semileptonically. The charged Higgs induced single-top process can be searched via  $pp \rightarrow bH^+ + X \rightarrow bt\bar{b} + X$  [68]<sup>2</sup>.

If cosmic inflation is realized in the g2HDM it may favor nearly degenerate  $A$ ,  $H$ ,  $H^\pm$  as shown in Refs. [73, 74]. It has been found that for mass and width degenerate  $A$  and  $H$  would lead to exact cancellation of the  $cg \rightarrow tA \rightarrow tt\bar{c}$  and  $cg \rightarrow tH \rightarrow tt\bar{c}$  amplitudes [58]. This would lead to diminished signature for the same-sign top signature while while no such cancellation exist for  $cg \rightarrow bH^+ \rightarrow bt\bar{b}$  and  $cg \rightarrow tA/tH \rightarrow tt\bar{t}$ . Therefore, vanishingly small same-sign signature but discovery of  $cg \rightarrow bH^+ \rightarrow bt\bar{b}$  and  $cg \rightarrow tA/tH \rightarrow tt\bar{t}$  may provide indirect evidence for inflation.

The paper is organized as follows. In Sec. II we discuss in detail the model framework and relevant constraints for the parameter space. We first start our discussion with the discovery prospect of the single-top i.e.  $pp \rightarrow bH^+ + X \rightarrow bt\bar{b} + X$  signature in Sec. III. The Sec. IV and Sec. V are dedicated for the same-sign top and triple-top signatures respectively. We close with implications of these discovery and a outlook in Sec. VI.

## II. FRAMEWORK PARAMETER SPACE

We consider the most general  $CP$ -conserving two Higgs doublet potential which is written in the Higgs basis as [75, 76]

$$V(\Phi, \Phi') = \mu_{11}^2 |\Phi|^2 + \mu_{22}^2 |\Phi'|^2 - (\mu_{12}^2 \Phi^\dagger \Phi' + h.c.) + \frac{\eta_1}{2} |\Phi|^4 + \frac{\eta_2}{2} |\Phi'|^4 + \eta_3 |\Phi|^2 |\Phi'|^2 + \eta_4 |\Phi^\dagger \Phi'|^2 + \left[ \frac{\eta_5}{2} (\Phi^\dagger \Phi')^2 + (\eta_6 |\Phi|^2 + \eta_7 |\Phi'|^2) \Phi^\dagger \Phi' + h.c. \right], \quad (1)$$

with the  $\eta_i$ s are the quartic couplings,  $\mu_{ij}$ s are dimension two mass parameters. The vacuum expectation value  $v$  arises from the  $\Phi$  doublet via the stationary condition  $\mu_{11}^2 = -\frac{1}{2}\eta_1 v^2$ , while  $\langle \Phi' \rangle = 0$  (hence  $\mu_{22}^2 > 0$ ). The second stationary condition is  $\mu_{12}^2 = \frac{1}{2}\eta_6 v^2$  and the

---

<sup>2</sup> For  $\bar{c}bH^+$  induced similar productions see also Refs. [69–72].

mixing angle  $\gamma$

$$c_\gamma^2 = \frac{\eta_1 v^2 - m_h^2}{m_H^2 - m_h^2}, \quad \sin 2\gamma = \frac{2\eta_6 v^2}{m_H^2 - m_h^2}. \quad (2)$$

diagonalizes the CP-even mass matrix of  $h$ ,  $H$ , and satisfies [75, 76] where we used shorthand for  $c_\gamma$  for  $\cos \gamma$ . In the alignment limit the  $\cos \gamma$  goes to zero limit. The masses of the neutral and charged scalars are found as

$$m_A^2 = \frac{1}{2}(\eta_3 + \eta_4 - \eta_5)v^2 + \mu_{22}^2, \quad (3)$$

$$m_{h,H}^2 = \frac{1}{2} \left[ m_A^2 + (\eta_1 + \eta_5)v^2 \mp \sqrt{(m_A^2 + (\eta_5 - \eta_1)v^2)^2 + 4\eta_6^2 v^4} \right], \quad (4)$$

$$m_{H^\pm}^2 = \frac{1}{2}\eta_3 v^2 + \mu_{22}^2. \quad (5)$$

The fermion interactions with the scalar bosons  $h$ ,  $H$ ,  $A$  and  $H^\pm$  is expressed as [75]

$$\begin{aligned} \mathcal{L} = & -\frac{1}{\sqrt{2}} \sum_{F=U,D,L} \bar{F}_i \left[ (-\lambda_{ij}^F s_\gamma + \rho_{ij}^F c_\gamma) h + (\lambda_{ij}^F c_\gamma + \rho_{ij}^F s_\gamma) H - i \operatorname{sgn}(Q_F) \rho_{ij}^F A \right] P_R F_j \\ & - \bar{U}_i [(V \rho^D)_{ij} P_R - (\rho^{U\dagger} V)_{ij} P_L] D_j H^+ - \bar{\nu}_i \rho_{ij}^L P_R L_j H^+ + \text{H.c.}, \end{aligned} \quad (6)$$

where  $V$  is the Cabibbo-Kobayashi-Maskawa (CKM) matrix and  $P_{L,R} \equiv (1 \mp \gamma_5)/2$  with  $i, j = 1, 2, 3$  are generation indices in flavor space. The  $U$ ,  $D$  and  $L$  denotes the matrices  $U = (u, c, t)$ ,  $D = (d, s, b)$ ,  $L = (e, \mu, \tau)$  and  $\nu = (\nu_e, \nu_\mu, \nu_\tau)$  whereas the matrices  $\lambda_{ij}^F$  ( $\equiv \delta_{ij} \sqrt{2} m_i^F / v$ ) and  $\rho_{ij}^F$  two Yukawa couplings. The  $\lambda^F$  matrices are real and diagonal but  $\rho^F$  matrices are in general in general nondiagonal and complex. The  $\rho_{ii}^F$  matrices may follow the same flavor organization principle as in SM i.e.  $\rho_{ii}^F \sim \lambda_i^F$  with suppressed off-diagonal elements which simply means  $\rho_{tt}^U \sim \lambda_t^U$ ,  $\rho_{bb}^D \sim \lambda_b^D$  etc. In what follows we drop the superscript  $F$  and set all  $\rho_{ij}$  couplings to zero except for  $\rho_{tt}$  and  $\rho_{tc}$  and assume them to be real for simplicity.

Our focus of interest is to study the discovery potential of the  $cg \rightarrow bH^+ \rightarrow bt\bar{b}$  (single-top),  $cg \rightarrow tA/tH \rightarrow tt\bar{c}$  (same-sign top) and  $cg \rightarrow tA/tH \rightarrow tt\bar{t}$  (triple-top) productions at the LHC and their respective implications for baryogenesis and inflation. The first and last processes are induced if both  $\rho_{tc}$  and  $\rho_{tt}$  are nonvanishing, whereas, the same-sign top is induced by the  $\rho_{tc}$  coupling alone. We remark here that similar final state topology can be induced by  $\rho_{tu}$  which we shall not cover in the current manuscript except for the same-sign top i.e.  $ug \rightarrow tA/tH \rightarrow tt\bar{u}$ . Here we assume  $\rho_{tc}$  and  $\rho_{tt}$  are real but the signatures discussed will remain unchanged if they are complex.

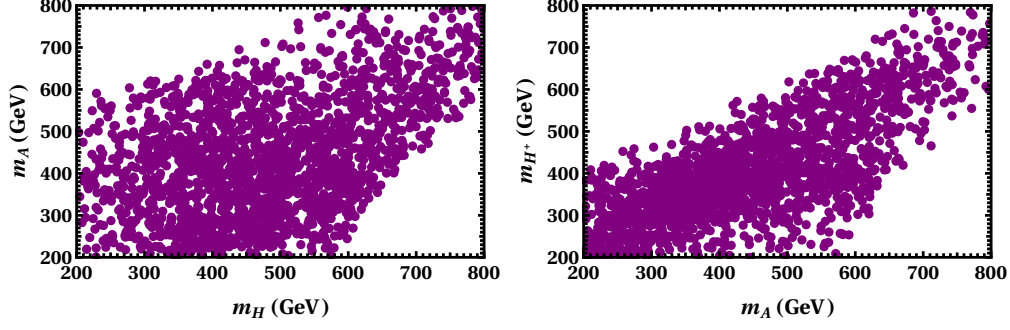


FIG. 1. The available parameter space that satisfy after satisfy positivity, perturbativity, tree-level unitarity and EW precision observables are plotted in the  $m_A$ - $m_H$  and  $m_A$ - $m_{H^+}$  plane.

Before exploring the discovery prospect let us first discuss the available parameter space. The dynamical parameters in Eq. (1) need to satisfy the positivity, perturbativity and tree-level unitarity. We check these constraints in the public tool 2HDMC [77] by first expressing the quartic couplings  $\eta_1, \eta_{3-6}$  in terms of  $m_h^2, m_{H^+}^2, m_A^2, m_H^2, \gamma, \mu_{22}^2$  and  $v$  as [75]

$$\eta_1 = \frac{m_h^2 s_\gamma^2 + m_H^2 c_\gamma^2}{v^2}, \quad (7)$$

$$\eta_3 = \frac{2(m_{H^+}^2 - \mu_{22}^2)}{v^2}, \quad (8)$$

$$\eta_4 = \frac{m_h^2 c_\gamma^2 + m_H^2 s_\gamma^2 - 2m_{H^+}^2 + m_A^2}{v^2}, \quad (9)$$

$$\eta_5 = \frac{m_H^2 s_\gamma^2 + m_h^2 c_\gamma^2 - m_A^2}{v^2}, \quad (10)$$

$$\eta_6 = \frac{(m_h^2 - m_H^2)(-s_\gamma)c_\gamma}{v^2}. \quad (11)$$

The quartic couplings  $\eta_2$  and  $\eta_7$  do not enter scalar masses. We generate the phenomenological parameters  $\gamma, m_A, m_H, m_{H^+}, \mu_{22}, \eta_2, \eta_7$  randomly in the following ranges:  $\mu_{22} \in [0, 1000]$  GeV,  $m_{H^+} \in [200, 800]$  GeV,  $m_A \in [200, 800]$  GeV,  $m_H \in [200, 800]$ ,  $\eta_2 \in [0, 5]$ ,  $\eta_7 \in [-5, 5]$ , with  $m_h = 125$  GeV and  $c_\gamma = 0$  held fixed. These randomly generated parameters are then fed into 2HDMC [77] for scanning in the Higgs basis<sup>3</sup>. We further demand the magnitude of all quartic couplings should be  $\leq 5$  conservatively. Further the constraints from precision electroweak observables [78] further restricts the parameter space [79, 80] which we have included in our analysis. The parameter sets that passed the positivity, perturbativity and tree-level unitarity conditions from 2HDMC, are also tested for the pre-

<sup>3</sup> The input parameters in the Higgs basis in 2HDMC are  $\Lambda_{1-7}$  and  $m_{H^+}$  with  $v \simeq 246$  GeV is implicit. In order to match the convention we take  $-\pi/2 \leq \gamma \leq \pi/2$  and identify  $\Lambda_{1-7}$  as  $\eta_{1-7}$ .

cision electroweak observables [81]. These final scanned points are plotted in the  $m_H-m_A$  and  $m_{H^+}-m_A$  in Fig. 1 which illustrates that finite sub-TeV parameter space still exist.

We now briefly discuss the constraints on  $\rho_{tc}$  and  $\rho_{tt}$ . There exists several indirect and direct constraints on  $\rho_{tc}$ . For nonzero  $c_\gamma$  the  $\rho_{tc}$  receives significant constraints from branching ratio of the  $t \rightarrow ch$  [82]. The ATLAS [83] and CMS [84] both set same 95% CL upper limit  $\mathcal{B}(t \rightarrow ch) < 9.4 \times 10^{-4}$  with full Run-2 data which is shown in Fig. 2 by purple shaded region. It is clear from Fig 2 that  $|\rho_{tc}| \gtrsim 0.8$  is excluded at 95% CL for  $c_\gamma \sim 0.1$ . The limit becomes stringent for larger  $c_\gamma$ .

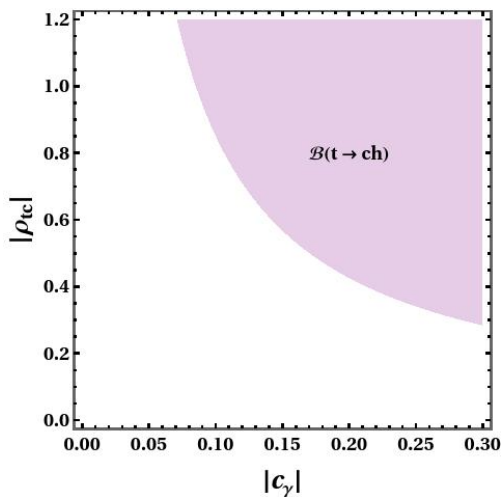


FIG. 2. Exclusion limits from  $\mathcal{B}(t \rightarrow ch) < 9.4 \times 10^{-4}$  in the for  $|\rho_{tc}|$ - $c_\gamma$  plane.

Further  $\rho_{tc}$  also receives more constraints albeit milder from  $B_s$ - $\bar{B}_s$  mixing and  $\mathcal{B}(B \rightarrow X_s \gamma)$  [85]. Such constraints arise through the loop of charm quarks and a charged Higgs involving  $\rho_{tc}$  but reinterpreting the limits from Ref. [86] one finds  $|\rho_{tc}| \gtrsim 0.9$  (1.2) is excluded at  $2\sigma$  for  $m_{H^+} = 300$  (500) GeV. However, the most stringent limit on  $\rho_{tc}$  arise from the CMS search for the SM four-top production [18], a discussion of which we defer to Sec. IV.

The  $\rho_{tt}$  is also constrained by indirect and direct measurements. E.g. the  $t\bar{t}h$  coupling measurement by ATLAS [87] and CMS [88] can constrain  $\rho_{tt}$  but weak [89]. This is primarily due to the suppression from the mixing angle  $c_\gamma$ , as can be seen from Eq. (6). However, the  $B_{s,d}$  mixing amplitude, where  $\rho_{tt}$  enters at one loop through  $tbH^\pm$  vertex, provides by far the most stringent limit with milder constraint also appears from  $B \rightarrow X_s \gamma$  ( $\mathcal{B}(B \rightarrow X_s \gamma)$ ) measurement. We plot the exclusion region for  $|\rho_{tt}|$  from  $B_{s,d}$  mixing by allowing  $2\sigma$  error on the UTfit values [90] in Fig. 3. The direct search limits from  $pp \rightarrow \bar{t}H^+(b) \rightarrow t\bar{t}\bar{b}(b)$  [48, 49]

are stronger than  $B_{s,d}$  mixings [68] specially for  $m_{H^\pm} \gtrsim 250$  GeV. We show the stronger CMS limit [49] by green shaded region in Fig. 3 assuming  $\mathcal{B}(H^\pm \rightarrow tb) = 100\%$ . The limits from  $pp \rightarrow H/A \rightarrow t\bar{t}$  [28, 29] and  $pp \rightarrow t\bar{t}H/A \rightarrow t\bar{t}t\bar{t}$  [18] are somewhat weaker than those from  $B_{s,d}$  mixings or  $m_{H^\pm}$  search [68].

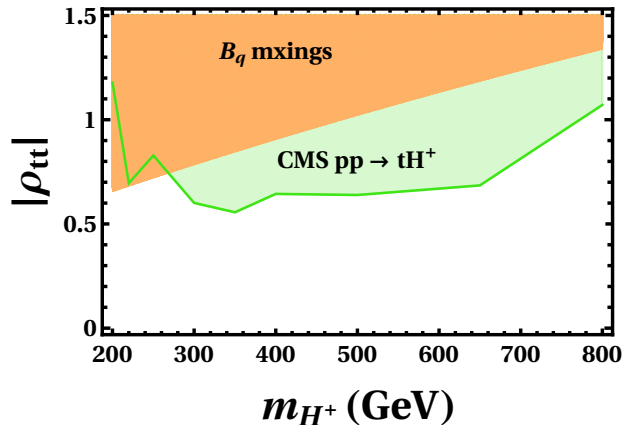


FIG. 3. Exclusion regions of  $\rho_{tt}$  from  $B_{s,d}$  mixings (orange) and CMS search of  $pp \rightarrow \bar{t}H^+(b) \rightarrow t\bar{t}\bar{b}(b)$  [49] (green) in the  $|\rho_{tt}|-m_{H^+}$  plane.

### III. CHARGED HIGGS INDUCED SINGLE-TOP PRODUCTION

First we discuss the discovery potential of  $cg \rightarrow bH^+$  followed by  $H^+ \rightarrow t\bar{b}$  decay [68]. The process is induced if  $\rho_{tc}$  and  $\rho_{tt}$  are non vanishing with both production and decay are  $V_{tb}$  proportional. At the LHC it can be searched via  $pp \rightarrow bH^+ + X \rightarrow bt\bar{b} + X$ , with subsequent decay of  $t \rightarrow b\ell\nu_\ell$ , constituting three  $b$ -jets, one charged lepton ( $\ell = e, \mu$ ), and missing transverse energy  $E_T^{\text{miss}}$  signature. Note that  $\rho_{tc}$  and  $\rho_{tt}$  coupling will also induce PDF suppressed  $bg \rightarrow \bar{c}H^+ \rightarrow \bar{c}t\bar{b}$  and,  $bg \rightarrow \bar{t}H^+ \rightarrow \bar{t}c\bar{b}$  which will contribute to the overall signature if the  $c$ -jet is misidentified as  $b$ -jet. Furthermore,  $\rho_{tt}$  can induce subdominant  $bg \rightarrow \bar{t}H^+ \rightarrow \bar{t}t\bar{b}$  process, which, with one top quark decaying semileptonically and other hadronically would also contribute to the same final state topology. We have accounted for all these contributions together in our analysis. We remark here that  $bg \rightarrow \bar{t}H^+ \rightarrow \bar{t}t\bar{b}$  is the usual search mode for  $H^\pm$  discovery for the ATLAS [46, 50] and CMS [47, 49] which is PDF suppressed in contrast to  $cg \rightarrow bH^+ \rightarrow bt\bar{b}$ .

The dominant SM backgrounds are QCD  $t\bar{t}$ +jets production and  $s$ - and  $t$ -channel single-top ( $tj$ ),  $Wt$  productions. The subdominant contributions also arise from  $t\bar{t}h$  and,  $t\bar{t}Z$

with negligible fractions come from  $Z/\gamma^*$ +jets, four-top ( $4t$ ), inclusive  $W$  production,  $t\bar{t}W$ ,  $tWh$ . We combine these subdominant and negligible contributions together and denote as “Others”.

We generate signal and background events at the leading order (LO) in Monte Carlo event generator MadGraph5\_aMC@NLO [91] (denoted as MadGraph5\_aMC) with the parton distribution function (PDF) set NN23LO1 [92] at  $\sqrt{s} = 14$  TeV. The generated events are then interfaced with PYTHIA [93, 94] for showering and hadronization. To incorporate the detector effects we utilized fast detector simulator Delphes 3 [95] on our analysis. The the matrix elements (ME) for the all the dominant and most subdominant backgrounds are generated with at least one additional jet, followed by ME and parton shower merging via MLM matching scheme [96, 97]. The jets are reconstructed with the anti- $k_t$  algorithm with radius parameter  $R = 0.5$ . The effective model is implemented is FeynRules [98].

The LO cross section of the  $t\bar{t}$ +jets background is normalized up to the NNLO by a factor 1.84 [99]. The  $s$ - and  $t$ -channel single-top productions are accounted up to the NNLO cross sections by factors 1.47 and 1.2 respectively [100] while  $Wt$ +jets cross section is adjusted up to the NLO by factor 1.35 [101]. Further, the subdominant  $t\bar{t}Z$  and  $t\bar{t}h$  cross sections are corrected to the corresponding NLO ones respectively by factors 1.56 [102] and 1.27 [103]. The  $Z/\gamma^*$ +jets background is normalized up to NNLO cross sections by factor 1.27 [104], whereas the tiny  $4t$  and  $t\bar{t}W$  backgrounds are up to NLO by factors 2.04 [91] and 1.35 [105] respectively. The backgrounds  $tWh$  and  $W$ +jets are kept at the LO. For simplicity the charge conjugate processes assumed to have the same correction factor throughout the paper and the signal cross sections are kept at LO. We take two benchmark masses  $m_{H^\pm} = 300$  and 500 GeV for with  $\rho_{tc} = 0.4$  and  $\rho_{tt} = 0.6$  for illustration.

To reduce the backgrounds following event selection cuts are applied. The events are selected such that they contain at least one lepton, at least three  $b$ -jets and some  $E_T^{\text{miss}}$ . The minimum transverse momentum ( $p_T$ ) of the leading lepton is required to be  $> 30$  GeV while for all three  $b$ -jets  $p_T > 20$  GeV. The maximum pseudo-rapidity ( $|\eta|$ ) for the of all three  $b$ -jets and the lepton should be  $< 2.5$ . The minimum separation ( $\Delta R$ ) between any  $b$ -jet and lepton and, between any two  $b$ -jets are needed to be  $> 0.4$ . In each event  $E_T^{\text{miss}}$  is required to be  $> 35$  GeV. Finally,  $H_T$ , defined as the sum of  $p_T$  of the leading three  $b$ -jets and the leading lepton, should be  $> 350$  GeV and  $> 400$  GeV respectively for  $m_{H^\pm} = 300$  and 500 GeV respectively.

Benchmark masses	$t\bar{t}+$ jets	Single-top	$Wt+$ jets	$t\bar{t}h$	$t\bar{t}Z$	Others	Total Bkg. (fb)
$m_{H^\pm} = 300$ GeV	1348.02	41.31	33.2	4.24	1.52	3.14	1431.43
$m_{H^\pm} = 500$ GeV	884.64	25	20.78	2.88	1.03	1.85	936.13

TABLE I. The background cross sections (in fb) of the different backgrounds of the  $pp \rightarrow bH^\pm + X \rightarrow bt\bar{b} + X$  process after selection cuts at  $\sqrt{s} = 14$  TeV [68].

Benchmark masses	Signal (fb)	Significance ( $\mathcal{Z}$ ) 300 (600) fb $^{-1}$
$m_{H^\pm} = 300$ GeV	12.5	5.7 (8.1)
$m_{H^\pm} = 500$ GeV	10.01	5.6 (8)

TABLE II. The signal cross sections of the  $bH^\pm$  process for  $m_{H^\pm} = 300$  and 500 GeV. The respective significances with 300 (600) fb $^{-1}$  integrated luminosities are given in third column [68].

We compute the significance using the likelihood formula for a simple counting experiment as [106]

$$Z(n|n_{\text{pred}}) = \sqrt{-2 \ln \frac{L(n|n_{\text{pred}})}{L(n|n)}}, \quad \text{with} \quad L(n|\bar{n}) = \frac{e^{-\bar{n}} \bar{n}^n}{n!}, \quad (12)$$

where  $n$  is the number of observed events and  $n_{\text{pred}}$  predicted events. For discovery, we perform hypothesis test between the observed signal plus background to the background prediction with  $Z(s+b|b) > 5$  is required for discovery. For exclusion limits we demand  $Z(b|s+b) > 2$ .

Let us discuss Table II and the discovery potential of  $bH^\pm$ . We found that, the achievable statistical significance for  $m_{H^\pm} = 300$  GeV is  $\sim 5.7\sigma$  and for  $m_{H^\pm} = 500$  GeV  $\sim 5.6\sigma$  at 300 fb $^{-1}$  integrated luminosity. This illustrates that full Run-3 data can discover the single-top signature while collected Run-2 data ( $\sim 137$  fb $^{-1}$ ) could reach to  $3.9\sigma$  and  $3.8\sigma$  significances.

#### IV. SAME-SIGN TOP

The  $\rho_{tc}$  coupling can induce  $cg \rightarrow tA/tH$ , followed by  $A/H \rightarrow t\bar{c}, \bar{t}c$  in g2HDM. The  $t\bar{t}c$  final state would be diminished by overwhelming QCD  $t\bar{t}$  production, however,  $t\bar{t}c$  followed by semileptonically decaying top quarks give exquisite same-sign dilepton signature. Such signature would provide an excellent probe for the  $\rho_{tc}$  coupling at the LHC. No dedicated same-sign search has been performed at the LHC however some existing searches of ATLAS and CMS can provide meaningful constraints. We note that  $\rho_{tc}$  coupling may also induce subdominant  $cg \rightarrow t\bar{t}c$  and  $t$ -channel  $H/A$  exchanged  $cc \rightarrow tt$  processes which we included in our analysis.

The search for SM  $4t$  production by CMS [18] based on  $137 \text{ fb}^{-1}$  data at  $\sqrt{s} = 13 \text{ TeV}$  can constrain the parameter space for same-sign top. The search has different signal (SRs) and control (CRs) regions based on the number of charged leptons ( $e, \mu$ ) and  $b$ -tagged jets [18]. It was shown that the or  $t\bar{t}W$  control region (denoted by CRW) [18] provides the best constraints for  $|\rho_{tc}|$  [59, 64–66].

As per the baseline selection criterion of Ref. [18], each event should contain two same-sign leptons and two  $b$ -jets and missing transverse momenta. The leading and subleading leptons are required to have  $p_T > 25$  and  $20 \text{ GeV}$  respectively with muon and electron  $|\eta| < 2.5$  (2.4). All jets should satisfy  $|\eta| < 2.4$ . In addition to these, the CRW region can have up to five jets with the rest of the selection cuts goes as follows: Events are selected if the  $p_T$  of the jets and  $b$ -jets fulfill any of the following three selection criteria [107]: (i) both the  $b$ -jets should have  $p_T > 40 \text{ GeV}$ ; (ii) one  $b$ -jet with  $p_T > 20 \text{ GeV}$  and  $20 < p_T < 40 \text{ GeV}$  for the second  $b$ -jet, but  $p_T > 40 \text{ GeV}$  for the third jet; (iii) both  $b$ -jets should satisfy  $20 < p_T < 40 \text{ GeV}$ , but with two extra jets each with  $p_T > 40 \text{ GeV}$ . The scalar sum of the  $p_T$  of all jets ( $H_T$ ) is required to be  $H_T > 300 \text{ GeV}$  and  $p_T^{\text{miss}} > 50 \text{ GeV}$ . To reduce the charge-misidentified Drell-Yan ( $Z/\gamma^*$ ) background CMS vetoed events with same-sign electron pairs lying within  $m_{ee} < 12 \text{ GeV}$ . With the above selection criteria  $335 \pm 18$  events were expected (SM backgrounds plus  $4t$ ) in the CRW while 338 events have been observed [18].

For sizable  $\rho_{tc}$  the  $cg \rightarrow tA/tH \rightarrow t\bar{t}c$  processes abundantly populate the CRW region leading to stringent constraints on  $\rho_{tc}$ . However, if  $H, A$  are nearly degenerate in mass and width strong cancellation between the  $cg \rightarrow tA \rightarrow t\bar{t}c$  and  $cg \rightarrow tH \rightarrow t\bar{t}c$  happen. The cancellation is exact if both mass and widths are degenerate [58]. This can be simply

understood from Eq.6, where the  $cg \rightarrow tA \rightarrow tt\bar{c}$  amplitude has an additional a factor of  $i^2 = -1$  to that  $cg \rightarrow tH \rightarrow tt\bar{c}$ . In order to avoid such cancellation and break the mass and width degeneracy we take  $|m_A - m_H| = 50$  GeV. Assuming  $\rho_{tc}$  is only non-vanishing coupling and demanding the sum of the  $\rho_{tc}$ -induced events and expected SM and agree with observed number of events within the  $2\sigma$  error bars we show the excluded region from CRW in Fig. 4 (left) green shaded regions. We also provide the constraint on  $\rho_{tu}$  for comparison. Here we assumed Gaussian behavior for simplicity.

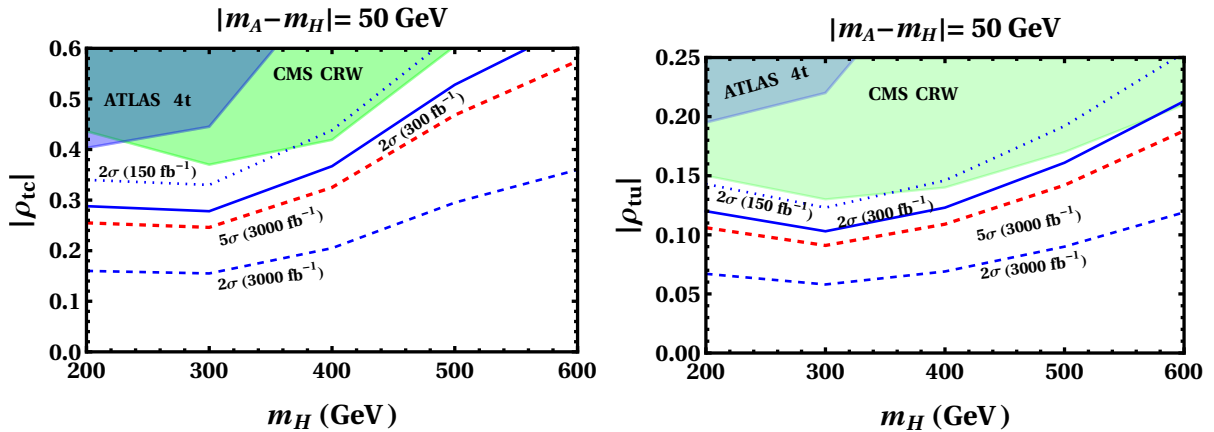


FIG. 4. Exclusion limits (blue) and discovery reaches (red) for  $|\rho_{tc}|$  and  $|\rho_{tu}|$  by the same-sign top signature for various integrated luminosities at the 14 TeV LHC. The purple and cyan regions are excluded respectively by CMS CRW [18] and ATLAS CRttW2 $\ell$  [16] control regions.

A similar  $4t$  search has been performed by ATLAS [30] with full Run-2 data but the selection criteria categorizing into different CRs and SRs are somewhat different from that of CMS. It has been found that the  $tt\bar{W}$ , called CRttW2 $\ell$  of Ref. [30] is the most relevant one. The CR is defined to have least two same-sign leptons ( $e\mu$  or  $\mu\mu$ ), at least four jets with at least two of them being  $b$ -tagged. For the same-sign leptons  $p_T > 28$  GeV with  $|\eta^\mu| < 2.5$  and  $|\eta^e| < 1.5$  whereas all the jets should satisfy  $p_T > 25$  GeV and  $|\eta| < 2.5$ . The scalar  $p_T$  sum over all jets and same-sign leptons (different from CMS),  $H_T < 500$  GeV.

Unlike CRW for CMS, ATLAS does provide the expected and observed events in CRttW2 $\ell$ , however, provide a figure of comparison between prediction and data for the variable  $\sum p_T^\ell$  (see Ref. [30] for detailed definition). Following Ref. [108] prescription of digitizing the figure, Ref. [64] found the number of expected and observed events in the CRttW2 $\ell$  from this distribution to be  $378 \pm 10$  and 380 respectively. Here errors for the

expected events in each bin of the  $\sum p_T^\ell$  distributions are simply added in quadrature. The exclusion region from CRttW2 $\ell$  is shown in Fig. 4 by blue shaded regions. Here we followed the same procedure as in before for event generation, hadronization, showering while utilized CMS based detector card of Delphes. At this point we remark that the ATLAS collaboration has made several similar searches [109, 110] constraints are much weaker due to strong selection cuts [65].

### A. A dedicated same-sign top search

Although the CMS and ATLAS  $4t$  search with Run 2 data can provide meaningful constraints, however, the searches are not optimized for  $cg \rightarrow tA/tH \rightarrow tt\bar{c}$  processes. Here we discuss a dedicated same-sign top search via  $pp \rightarrow tA/tH + X \rightarrow tt\bar{c} + X$  followed by semileptonic decay of both the top quarks with two same-sign dileptons ( $e, \mu$ ), three jets with at least two  $b$ -tagged jets and missing energy. We denote this signature as SS2 $l$ -2 $bj$ .

There are several SM backgrounds for SS2 $l$ -2 $bj$  topology. The dominant ones are  $t\bar{t}W$ ,  $t\bar{t}Z$ ,  $4t$ ,  $tZ$ +jets and  $t\bar{t}h$ . Further if a lepton charge is misidentified (denoted as charge- or  $Q$ -flip) the  $t\bar{t}$ +jets and  $Z/\gamma^*$ +jets processes would also contribute to the overall background cross section with a misidentification efficiency  $2.2 \times 10^{-4}$  [111–113]. A CMS study [114] with similar final state topology, albeit slightly different selection cuts, reported the “nonprompt” and fake backgrounds are that of  $\sim 1.5$  times the  $t\bar{t}W$  background. As the nonprompt and fake backgrounds are not ideally modeled in Monte Carlo simulations, for simplicity we just add this component to the overall background at 1.5 times that of  $t\bar{t}W$  background after our selection cuts. There of course are some tiny backgrounds, such as  $3t + W$  and  $3t + j$  etc. which we have neglected in our analysis. For event generation, hadronization, showering and detector effects we follow the same simulation chains as in previous section. Moreover we utilize the same  $K$  factors for different backgrounds as described earlier while keep the signal cross sections at LO.

We adopt following selection cuts for the SS2 $l$ -2 $bj$  search [64, 65]. The leading and subleading leptons are need to have  $p_T > 25$  and 20 GeV respectively, while pseudo rapidity should be  $|\eta| < 2.5$ . The jets are required to have  $p_T > 20$  GeV and  $|\eta| < 2.5$  with  $E_T^{\text{miss}} > 35$  GeV. The  $\Delta R$  between any two visible objects should satisfy  $\Delta R > 0.4$ . Finally, we apply scalar sum of the  $p_T$  of the two same-sign leptons and two leading  $b$ -tagged jets and the

Backgrounds	Cross section (fb)
$t\bar{t}W$	1.31
$t\bar{t}Z$	1.97
$4t$	0.316
$tZ$ + jets	0.255
$t\bar{t}h$	0.07
$Q$ -flip	0.024
nonprompt	$1.5 \times t\bar{t}W$

TABLE III. The background cross sections for a dedicated SS2l-2bj search.

leading non  $b$ -tagged jets should be  $> 300$  GeV. The background cross sections with the above selection cuts are provided in Table III. We estimate the signal cross sections for a reference  $\rho_{tc} = 1$  for few discrete values of  $m_H$  with  $|m_A - m_H| = 50$  GeV and assuming  $m_H > m_A$  with  $\mathcal{B}(A/H \rightarrow t\bar{c} + \bar{t}c) = 100\%$ . We then scale the signal cross section simply with  $|\rho_{tc}|^2 \mathcal{B}(A/H \rightarrow t\bar{c} + \bar{t}c)$  and provide discovery (red) and exclusion (blue) contours for in Fig. 4. A similar procedure is repeated for  $\rho_{tu}$  induced SS2l-2bj for the right panel of Fig. 4. For a detail discussion on SS2l-2bj we redirect readers to Refs. [64, 65].

Let us understand the Fig. 4. A dedicated SS2l-2bj search could exclude  $|\rho_{tc}| \sim 0.5$  for  $m_H \sim 200$ –400 GeV with  $|\rho_{tc}| \sim 0.6$ –0.7 for  $m_H \sim 500$ –700 GeV. More stringent limit is achievable with full Run-3 data while high luminosity LHC (HL-LHC) i.e. with full 3000  $\text{fb}^{-1}$  integrated luminosity one  $|\rho_{tc}| \sim 0.1$  can be excluded for  $m_H \sim 200$ –400 GeV whereas reaching up to  $|\rho_{tc}| \sim 0.2$  for  $m_H \sim 500$ –700 GeV. A sensitive is possible for  $\rho_{tu}$  induced same-sign top signature, as can be seen from left panel of Fig. 4. Note here we set all other couplings to zero except for  $\rho_{tc}$  which simply leads same decay widths for  $A$  and  $H$ . If the mass difference  $|m_A - m_H|$  is reduced the  $cg \rightarrow tA \rightarrow t\bar{t}\bar{c}$  and  $cg \rightarrow tH \rightarrow t\bar{t}\bar{c}$  amplitudes will cancel each other making the same-sign top signature diminished.

## V. TRIPLE TOP

The triple-top signature  $cg \rightarrow tA/tH \rightarrow tt\bar{t}$  is induced if both  $\rho_{tc}$  and  $\rho_{tt}$  are nonzero. This process can be searched at the LHC via  $pp \rightarrow tA/tH + X \rightarrow tt\bar{t} + X$  with at least three leptons ( $\ell = e, \mu$ ) and three  $b$ -jets and  $E_T^{\text{miss}}$ . We remark that unlike the same-sign top signature the  $pp \rightarrow tA + X \rightarrow tt\bar{t} + X$  and  $pp \rightarrow tH + X \rightarrow tt\bar{t} + X$  processes do not cancel each other when both masses and decay widths are degenerate, the consequence of which we shall discuss shortly. This is because for a real  $\rho_{tt}$ , the  $cg \rightarrow tA \rightarrow tt\bar{t}$  amplitude gains a factor of  $i^2\gamma_5$  to that of the  $cg \rightarrow tH \rightarrow tt\bar{t}$  [58].

The dominant SM backgrounds as in before are  $t\bar{t}Z$ +jets,  $t\bar{t}W$ +jets,  $4t$  with subdominant contributions come from  $t\bar{t}h$ ,  $tZ$ +jets,  $t\bar{t}h$ ,  $3t + j$  and  $3t + W$ . The overwhelming  $t\bar{t}$ +jets process also contributes to the overall background contribution if one of the jet gets misidentified as a charged lepton. As discussed above such backgrounds are not properly modeled in Monte Carlo event generator such as MadGraph5\_aMC. Therefore we estimate such contribution by simply applying the selection cuts on the  $t\bar{t}$ +jets samples with one of the jet is taken as the third lepton with misidentification efficiency  $\epsilon_{\text{fake}} = 10^{-4}$  [112, 115]. The QCD  $K$  factors for different backgrounds are same as in previous sections with  $3t + j$  and  $3t + W$  and signal are kept at LO for simplicity.

In order to distinguish the signal events from the backgrounds following event selection cuts are applied. The events are selected such it contain at least three leptons, at least  $b$ -jets three and  $E_T^{\text{miss}}$ . The three leading  $b$ -jets and leptons are required to have  $p_T^\ell > 20$  GeV and  $p_T^b > 20$  GeV respectively and  $E_T^{\text{miss}} > 30$  GeV. The pseudo-rapidity . We further use the scalar sum of transverse momenta of the three leading  $b$ -jets and three leading leptons should be  $> 300$  GeV. Finally, to reduce contributions from  $t\bar{t}Z$ + and  $tZ$ -jets backgrounds, we reject events when a same flavor, opposite charged lepton pair lie within  $80 \text{ GeV} < m_{\ell\ell} < 100 \text{ GeV}$  window. For events, if more than one such pair exist the veto is applied to the pair to  $m_Z$ .

The signal and background cross sections are presented in Table V and Table IV. It is clear that triple top signature can be discovered at the HL-LHC provided  $\rho_{tc} \sim 1$  and  $\rho_{tt} \sim 1$  while evidence might come with  $600 \text{ fb}^{-1}$ . It may seem that  $\rho_{tc} \sim 1$  is excluded from the left panel Fig. 4, however, the exclusion region was found assuming all other couplings are vanishingly small. However, it is shown that an  $\mathcal{O}(1)$  is still allowed if  $\rho_{tt} \sim 1$ , where the latter coupling will suppress the same-sign top cross section via  $A/H \rightarrow t\bar{t}$  decay [66].

$t\bar{t}Z$	$4t$	$t\bar{t}W$	Others	$t\bar{t}$ +jets	Total Bkg. (fb)
0.135	0.105	0.011	0.007	0.1660	0.424

TABLE IV. Different background cross sections for triple-top signature. In the last column the total background cross sections is presented.

Benchmark masses	Signal (fb)	Significance ( $\mathcal{Z}$ ) 600 (3000) fb <sup>-1</sup>
$m_H = m_A = 400$ GeV	0.075	2.7 (6.1)
$m_H = m_A = 500$ GeV	0.063	2.3 (5.2)

TABLE V. The signal cross sections of the triple-top process for two different benchmark masses. The respective significances with 600 (3000) fb<sup>-1</sup> integrated luminosities are given in third column.

We now remark on the consequence of the discovery of the different heavy Higgs induced multi-top productions in the light of EWBG and inflation. It is found that complex  $10^{-2} \lesssim \rho_{tt} \gtrsim 1$  and  $\rho_{tc} \gtrsim 0.5$  [52] individually can account for the observed baryon asymmetry of the Universe. Therefore, it is clear that  $cg \rightarrow bH^+ \rightarrow bt\bar{b}$ ,  $cg \rightarrow tA/tH \rightarrow tt\bar{c}$  and  $cg \rightarrow tA/tH \rightarrow tt\bar{t}$  all could provide potential discovery mode for  $\rho_{tc}$  and  $\rho_{tt}$  EWBG mechanism. If inflation is realized in g2HDM it would require a nearly mass spectra for  $m_A$ ,  $m_H$ ,  $m_{H^\pm}$  [73, 74]. With nonvanishing  $\rho_{tc}$  and  $\rho_{tt}$ , for such a parameter space, the same  $cg \rightarrow bH^+ \rightarrow bt\bar{b}$  signature would emerge first but the same-sign top signature could be diminished significantly due to cancellation for near degeneracy of masses and widths [73, 74]. On the other hand the triple-top signature will also emerge providing a smoking gun signature for cosmic inflation.

## VI. SUMMARY AND OUTLOOK

We have discussed the discovery prospect of heavy Higgs induced single-top, same-sign, and triple-top productions in g2HDM. We have shown that for sizable  $\rho_{tc}$  and  $\rho_{tt}$  the  $cg \rightarrow bH^+ \rightarrow bt\bar{b}$  and  $cg \rightarrow tA/tH \rightarrow tt\bar{c}$  processes could be discovered with Run-3 data but  $cg \rightarrow tA/tH \rightarrow tt\bar{t}$  may require HL-LHC data. We have shown that the  $cg \rightarrow bH^+ \rightarrow bt\bar{b}$  could be discovered in the Run-3 if  $m_{H^\pm} \sim 200\text{--}500$  GeV. Existing ATLAS and CMS data provide some constraint but a dedicated search for the  $cg \rightarrow tA/tH \rightarrow tt\bar{c}$  should be performed. The Run-3 data may already provide sensitive probe for the same-sign top process if  $m_A$  and  $m_H$  lie in the 200–800 GeV range.

We have turned off all  $\rho_{ij}$  couplings except for  $\rho_{tt}$  and  $\rho_{tc}$  for simplicity. If  $\rho_{ii} \sim \lambda_i$  i.e.  $\rho_{bb} \sim \lambda_b$  and  $\rho_{\tau\tau} \sim \lambda_\tau$  different decay modes of  $A$ ,  $H$ ,  $H^\pm$  would open up. This would dilute the signatures mildly as long as these couplings are small. In general  $\rho_{bb} \sim 0.2$  is still allowed [57] while  $\rho_{tu} \sim 0.1$  is possible [64] for the sub-TeV  $A$ ,  $H$ ,  $H^\pm$ . Presence of such large couplings may not only dilute the signatures significantly the parameter space could also be subjected to several flavor physics observables [86]. This would require a detail analysis which we leave out for future.

The heavy Higgs induced single-top, same-sign top and triple-top signatures may provide indirect probes to baryogenesis and inflation. While both these early Universe phenomena are connected to sub-TeV mass range, however, the parameter space are mutually exclusive [73, 74]. It should be noted that the triple-top process is already covered in the search program of ATLAS collaboration [67]. We also highlight a dedicated webpage for the same-sign and triple-top processes for experimental studies [116] and similar page is being created for the charged Higgs induced single-top process. If discovered these processes would not only confirm beyond the Standard Model physics but may shed light on the mechanisms behind observed baryon asymmetry or the cosmic inflation.

**Acknowledgments** TM is supported by postdoctoral fellowship of Universität Heidelberg.

- 
- [1] V. Khachatryan *et al.* [CMS], Phys. Lett. B **695**, 424-443 (2011).
  - [2] G. Aad *et al.* [ATLAS], Eur. Phys. J. C **71**, 1577 (2011).
  - [3] G. Aad *et al.* [ATLAS], Phys. Lett. B **717**, 330-350 (2012).

- [4] S. Chatrchyan *et al.* [CMS], JHEP **12**, 035 (2012).
- [5] M. Aaboud *et al.* [ATLAS], JHEP **04**, 086 (2017).
- [6] A. M. Sirunyan *et al.* [CMS], Phys. Lett. B **772**, 752-776 (2017)
- [7] S. Chatrchyan *et al.* [CMS], Phys. Rev. Lett. **112**, no.23, 231802 (2014).
- [8] G. Aad *et al.* [ATLAS], JHEP **01**, 064 (2016).
- [9] M. Aaboud *et al.* [ATLAS], JHEP **01**, 063 (2018).
- [10] A. Tumasyan *et al.* [CMS], JHEP **11**, 111 (2021).
- [11] G. Aad *et al.* [ATLAS], Phys. Lett. B **756**, 228-246 (2016).
- [12] V. Khachatryan *et al.* [CMS], JHEP **09**, 027 (2016).
- [13] [ATLAS], [arXiv:2209.08990 [hep-ex]].
- [14] V. Barger, W. Y. Keung and B. Yencho, Phys. Lett. B **687**, 70-74 (2010).
- [15] M. Aaboud *et al.* [ATLAS], Phys. Rev. D **99**, 052009 (2019).
- [16] [ATLAS], ATLAS-CONF-2020-013.
- [17] A. M. Sirunyan *et al.* [CMS], Eur. Phys. J. C **78**, 140 (2018).
- [18] A. M. Sirunyan *et al.* [CMS], Eur. Phys. J. C **80**, no.2, 75 (2020)
- [19] A. Djouadi, Phys. Rept. **459**, 1-241 (2008).
- [20] G. C. Branco, P. M. Ferreira, L. Lavoura, M. N. Rebelo, M. Sher and J. P. Silva, Phys. Rept. **516**, 1-102 (2012).
- [21] G. Aad *et al.* [ATLAS Collaboration], Phys. Lett. B **716**, 1 (2012); S. Chatrchyan *et al.* [CMS Collaboration], *ibid.* B **716**, 30 (2012).
- [22] K. J. F. Gaemers and F. Hoogeveen, Phys. Lett. B **146**, 347-349 (1984).
- [23] D. Dicus, A. Stange and S. Willenbrock, Phys. Lett. B **333**, 126-131 (1994).
- [24] W. Bernreuther, M. Flesch and P. Haberl, Phys. Rev. D **58**, 114031 (1998).
- [25] R. Frederix and F. Maltoni, JHEP **01**, 047 (2009).
- [26] M. Carena and Z. Liu, JHEP **11**, 159 (2016).
- [27] D. Buarque Franzosi, E. Vryonidou and C. Zhang, JHEP **10**, 096 (2017).
- [28] M. Aaboud *et al.* [ATLAS], Phys. Rev. Lett. **119**, 191803 (2017).
- [29] A. M. Sirunyan *et al.* [CMS], JHEP **04**, 171 (2020).
- [30] G. Aad *et al.* [ATLAS], Eur. Phys. J. C **80**, 1085 (2020).
- [31] N. Craig, F. D'Eramo, P. Draper, S. Thomas and H. Zhang, JHEP **06**, 137 (2015).
- [32] S. Kanemura, H. Yokoya and Y.-J. Zheng, Nucl. Phys. B **898**, 286 (2015);

- [33] S. Gori, I.W. Kim, N.R. Shah and K.M. Zurek, Phys. Rev. D **93**, 075038 (2016);
- [34] N. Craig, J. Hajer, Y. Y. Li, T. Liu and H. Zhang, JHEP **01**, 018 (2017).
- [35] T. Plehn, Phys. Rev. D **67**, 014018 (2003).
- [36] J. F. Gunion and H. E. Haber, Phys. Rev. D **67**, 075019 (2003).
- [37] E. Boos and T. Plehn, Phys. Rev. D **69**, 094005 (2004).
- [38] A. G. Akeroyd, M. Aoki, A. Arhrib, L. Basso, I. F. Ginzburg, R. Guedes, J. Hernandez-Sanchez, K. Huitu, T. Hurth and M. Kadastik, *et al.* Eur. Phys. J. C **77**, 276 (2017).
- [39] N. Craig and S. Thomas, JHEP **11**, 083 (2012).
- [40] M. Carena, S. Heinemeyer, O. Stål, C. E. M. Wagner and G. Weiglein, Eur. Phys. J. C **73**, 2552 (2013).
- [41] M. Carena, I. Low, N. R. Shah and C. E. M. Wagner, JHEP **04**, 015 (2014).
- [42] D. de Florian *et al.* [LHC Higgs Cross Section Working Group],
- [43] R. Harlander, M. Kramer and M. Schumacher, [arXiv:1112.3478 [hep-ph]].
- [44] V. Khachatryan *et al.* [CMS], JHEP **11**, 018 (2015).
- [45] G. Aad *et al.* [ATLAS], JHEP **03**, 127 (2016).
- [46] M. Aaboud *et al.* [ATLAS], JHEP **11**, 085 (2018).
- [47] A.M. Sirunyan *et al.* [CMS], JHEP **01**, 096 (2020).
- [48] [ATLAS], ATLAS-CONF-2020-039.
- [49] A. M. Sirunyan *et al.* [CMS], JHEP **07**, 126 (2020).
- [50] G. Aad *et al.* [ATLAS], JHEP **06**, 145 (2021).
- [51] C. W. Chiang, K. Fuyuto and E. Senaha, Phys. Lett. B **762**, 315-320 (2016).
- [52] K. Fuyuto, W.-S. Hou and E. Senaha, Phys. Lett. B **776**, 402 (2018).
- [53] J. de Vries, M. Postma, J. van de Vis and G. White, JHEP **01**, 089 (2018).
- [54] J.M. Cline and B. Laurent, Phys. Rev. D **104**, 083507 (2021).
- [55] K. Enomoto, S. Kanemura and Y. Mura, JHEP **01**, 104 (2022).
- [56] K. Enomoto, S. Kanemura and Y. Mura, JHEP **09**, 121 (2022).
- [57] T. Modak and E. Senaha, Phys. Rev. D **99**, 115022 (2019).
- [58] M. Kohda, T. Modak, W.-S. Hou, Phys. Lett. B **776**, 379 (2018).
- [59] W.-S. Hou, M. Kohda, T. Modak, Phys. Lett. B **786**, 212 (2018).
- [60] W.-S. Hou, G.-L. Lin, C.-Y. Ma, C.-P. Yuan, Phys. Lett. B **409**, 344 (1997).
- [61] W. Altmannshofer, J. Eby, S. Gori, M. Lotito, M. Martone and D. Tuckler, Phys. Rev. D

- 94**, 115032 (2016).
- [62] S. Iguro and K. Tobe, Nucl. Phys. B **925**, 560-606 (2017).
- [63] W. Altmannshofer, B. Maddock and D. Tuckler, Phys. Rev. D **100**, 015003 (2019).
- [64] W.-S. Hou, T.-H. Hsu and T. Modak, Phys. Rev. D **102**, 055006 (2020).
- [65] W. S. Hou and T. Modak, Mod. Phys. Lett. A **36**, 2130006 (2021).
- [66] W.-S. Hou, M. Kohda and T. Modak, Phys. Lett. B **798**, 134953 (2019).
- [67] [ATLAS], ATLAS-CONF-2022-039.
- [68] D.K. Ghosh, W.-S. Hou and T. Modak, Phys. Rev. Lett. **125**, 221801 (2020).
- [69] J. L. Diaz-Cruz, J. Hernandez-Sanchez, S. Moretti, R. Noriega-Papaqui and A. Rosado, Phys. Rev. D **79**, 095025 (2009).
- [70] S. Gori, C. Grojean, A. Juste and A. Paul, JHEP **01**, 108 (2018)
- [71] U. Nierste, M. Tabet and R. Ziegler, Phys. Rev. Lett. **125**, 031801 (2020)
- [72] N. Desai, A. Mariotti, M. Tabet and R. Ziegler, JHEP **11**, 112 (2022).
- [73] S. M. Lee, T. Modak, K. y. Oda and T. Takahashi, Eur. Phys. J. C **82**, 18 (2022).
- [74] T. Modak and K. y. Oda, Eur. Phys. J. C **80**, 863 (2020).
- [75] See, e.g., S. Davidson and H.E. Haber, Phys. Rev. D **72**, 035004 (2005).
- [76] W. S. Hou and M. Kikuchi, EPL **123**, 11001 (2018).
- [77] D. Eriksson, J. Rathsman and O. Stål, Comput. Phys. Commun. **181**, 189 (2010).
- [78] M.E. Peskin and T. Takeuchi, Phys. Rev. D **46**, 381 (1992).
- [79] C.D. Froggatt, R.G. Moorhouse and I.G. Knowles, Phys. Rev. D **45**, 2471 (1992).
- [80] H.E. Haber and O. Stål, Eur. Phys. J. C **75**, 491 (2015).
- [81] M. Baak *et al.* [Gfitter Group], Eur. Phys. J. C **74**, 3046 (2014). The latest values of oblique parameters are obtained from Gfitter website: [http://project-gfitter.web.cern.ch/project-gfitter/Oblique\\_Parameters/](http://project-gfitter.web.cern.ch/project-gfitter/Oblique_Parameters/)
- [82] W.-S. Hou, Phys. Lett. B **296**, 179 (1992).
- [83] [ATLAS], [arXiv:2208.11415 [hep-ex]].
- [84] A. Tumasyan *et al.* [CMS], JHEP **02**, 169 (2022).
- [85] B. Altunkaynak, W.-S. Hou, C. Kao, M. Kohda and B. McCoy, Phys. Lett. B **751**, 135 (2015).
- [86] A. Crivellin, A. Kokulu, C. Greub, Phys. Rev. D **87**, 094031 (2013).
- [87] M. Aaboud *et al.* [ATLAS], Phys. Lett. B **784**, 173-191 (2018).

- [88] A.M. Sirunyan *et al.* [CMS], Phys. Rev. Lett. **120**, 231801 (2018).
- [89] W.-S. Hou, M. Kohda and T. Modak, Phys. Rev. D **98**, 075007 (2018).
- [90]  $B_{d,s}$  measurements of UFit collaboration, <http://www.utfit.org/UTfit/ResultsSummer2018NP>.
- [91] J. Alwall *et al.*, JHEP **1407**, 079 (2014).
- [92] R.D. Ball *et al.* [NNPDF], Nucl. Phys. B **877**, 290 (2013).
- [93] T. Sjöstrand, S. Mrenna and P. Skands, JHEP **0605**, 026 (2006).
- [94] T. Sjöstrand, S. Ask, J. R. Christiansen, R. Corke, N. Desai, P. Ilten, S. Mrenna, S. Prestel, C. O. Rasmussen and P. Z. Skands, Comput. Phys. Commun. **191**, 159-177 (2015).
- [95] J. de Favereau *et al.* [DELPHES 3], JHEP **1402**, 057 (2014).
- [96] M.L. Mangano, M. Moretti, F. Piccinini and M. Treccani, JHEP **0701**, 013 (2007).
- [97] J. Alwall *et al.*, Eur. Phys. J. C **53**, 473 (2008).
- [98] A. Alloul, N.D. Christensen, C. Degrande, C. Duhr and B. Fuks, Comput. Phys. Commun. **185**, 2250 (2014).
- [99] <https://twiki.cern.ch/twiki/bin/view/LHCPhysics/TtbarNNLO>.
- [100] <https://twiki.cern.ch/twiki/bin/view/LHCPhysics/SingleTopRefXsec>.
- [101] N. Kidonakis, Phys. Rev. D **82**, 054018 (2010).
- [102] J. Campbell, R.K. Ellis and R. Rötsch, Phys. Rev. D **87**, 114006 (2013).
- [103] <https://twiki.cern.ch/twiki/bin/view/LHCPhysics/CERNYellowReportPageAt14TeV2010>.
- [104] Y. Li and F. Petriello, Phys. Rev. D **86**, 094034 (2012).
- [105] J.M. Campbell and R.K. Ellis, JHEP **1207**, 052 (2012).
- [106] G. Cowan *et al.*, Eur. Phys. J. C **71**, 1554 (2011).
- [107] We thank K.-F. Chen for clarifications on this point.
- [108] C. Bonilla, T. Modak, R. Srivastava and J. W. F. Valle, Phys. Rev. D **98**, 095002 (2018).
- [109] G. Aad *et al.* [ATLAS], JHEP **06**, 046 (2020).
- [110] M. Aaboud *et al.* [ATLAS], JHEP **12**, 039 (2018).
- [111] The ATLAS collaboration, ATLAS-CONF-2016-037.
- [112] E. Alvarez, D.A. Faroughy, J.F. Kamenik, R. Morales and A. Szykman, Nucl. Phys. B **915**, 19 (2017).
- [113] M. Aaboud *et al.* [ATLAS], JHEP **1812**, 039 (2018).
- [114] A. M. Sirunyan *et al.* [CMS], Eur. Phys. J. C **77**, 578 (2017).
- [115] G. Aad *et al.* [ATLAS], Eur. Phys. J. C **76**, 259 (2016).

- [116] The model files and details for experimental studies of the same-sign and triple-top process:  
<https://twiki.org/cgi-bin/view/Sandbox/FlavorChangingNeutralHiggs>